CDF/PHYS/EXO/PUBLIC/10374

Search for Production of Top Quark Pairs Plus Invisible Particles at CDF.

The CDF Collaboration
URL http://www-cdf.fnal.gov
(Dated: February 3, 2011)

We present a search for dark matter particles in the decay of exotic 4th generation quarks t' which decay via $t' \to t + X$, where X is a dark matter particle. In a data sample with 4.8 fb^{-1} of integrated luminosity collected by the CDF experiment in $p\bar{p}$ collisions with $\sqrt{s} = 1.96$ TeV we search for pair production of T' in the lepton+jets channel, $p\bar{p} \to t\bar{t} + X + X \to \ell\nu bqq'b + X + X$. To isolate the detector signature of $\ell + 4$ jets $+ \not\!\!E_T$, we select events with an electron or muon, at least 4 jets and large missing transverse energy (100-160 GeV). Current direct and indirect bounds on such exotic quarks restrict their masses to be between 300 and 600 GeV, and the dark matter's mass anywhere below $m_{T'}$. The data are consistent with standard model expectations, and we set 95% confidence level limits on the production of $t\bar{t} + X + X$, which can be applied to T' production, or supersymmetric $\tilde{t} \to t + \chi^0$.

I. INTRODUCTION

We present a search for production of top quark pairs plus invisible particles using the CDF detector [1]. The model we investigate with top quark pairs and invisible particles involves exotic 4th generation quarks t' decaying via

$$t' \to t + X,$$

where X is dark matter [3]. We frame the analysis generically as a search for top quark pairs plus invisible particles, and reinterpret the results in terms of stop quarks decaying to top quarks plus stable neutral supersymmetric particles.

II. SIGNAL AND SELECTION

In the lepton + jets channel the detector signature is $t\bar{t} + \not\!\!E_T$, giving $\ell + \nu + qq' + bb' + \not\!\!E_T$, see Figure 1.

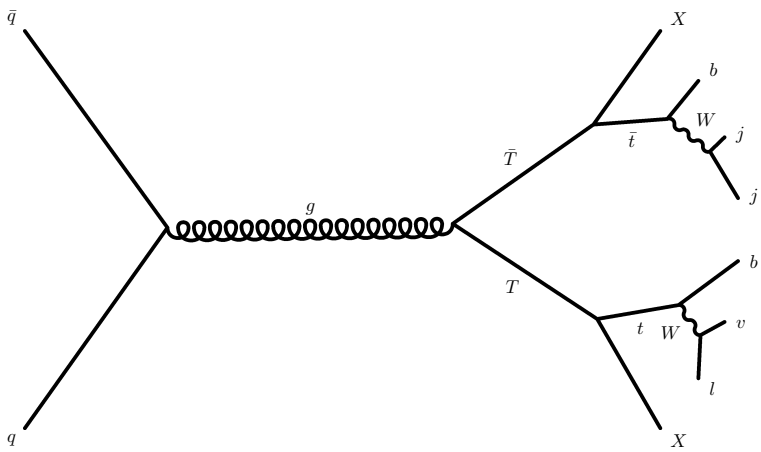

FIG. 1: Feynman diagram of signal event.

The amount of missing transverse momentum is characterized by two parameters: $m_{T'}$, mass of the fourth generation quark, and m_X, mass of the dark matter particle. Our analysis is two-dimensional as we probe sensitivity to signals for a range in $(m_{T'}, m_X)$. Current direct and indirect bounds restrict 300 GeV $\leq m_{T'} \leq$ 600 GeV [3].

Our signal is characterized by an excess $\not{E}_T$ due to the dark matter particles; to isolate large $\not{E}_T$ events with one lepton plus jets final state we require:

- Exactly one tight electron or muon with p_T >20GeV
- At least 4 jets with E_T >20GeV and $|\eta| < 2.0$
- $\not{E}_T \geq 100 - 160$ GeV. The $\not{E}_T$ in an event will be larger for signal points with larger $m'_T - m_X$, thus signal points with large $m'_T - m_X$ will have a higher optimal $\not{E}_T$ cut. The optimal $\not{E}_T$ cut depends on (m'_T, m_X) and have been listed in Table II.

III. MODELING AND BACKGROUNDS

We model the T' signal using MADGRAPH [2] to describe the hard process and PYTHIA [4] for the showering. The dominant backgrounds with our selection are $t\bar{t}$ and W+jets. The $t\bar{t}$ and dibsoson background samples are generated using PYTHIA, W+jets and Z+jets using ALPGEN [5]+PYTHIA, and the QCD sample is modeled from jet events in the data.

We validate our background in two control regions:

- High $\not{E}_T$ control region: $N_{jets} = 3$, $\not{E}_T > 100$ GeV: this validates the modeling of the large $\not{E}_T$ events which are the signature of the signal. This control region is depleted in signal due to the restriction on the number of jets.
- Low $\not{E}_T$ control region: $N_{jets} \geq 4$ and $\not{E}_T < 100$ GeV: this validates our modeling of events with 4-jets. This control region is depleted in signal due to the small $\not{E}_T$.

Our signal region is then defined as $N_{jets} \geq 4$ and $\not{E}_T > 100 - 160$ GeV.

We consider several sources of systematic uncertainty, including jet energy scale, contributions from additional interactions, uncertainty in descriptions of initial and final state radiation.

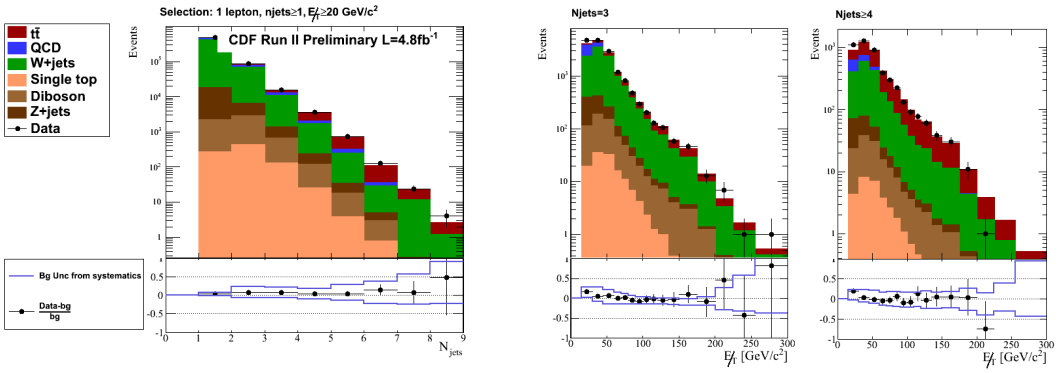

(a) N_{jets} with lepton+jets selection.

(b) $\not\!\!E_T$ with $N_{jets} = 3$ and $N_{jets} \geq 4$.

FIG. 2: Backgrounds vs data in N_{jets} and $\not\!\!E_T$.

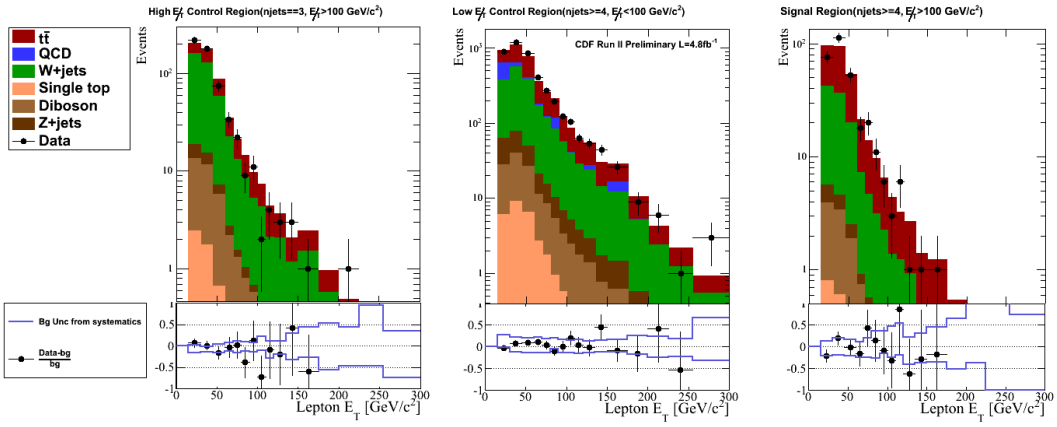

FIG. 3: Backgrounds vs data in lepton E_T with three different selections.

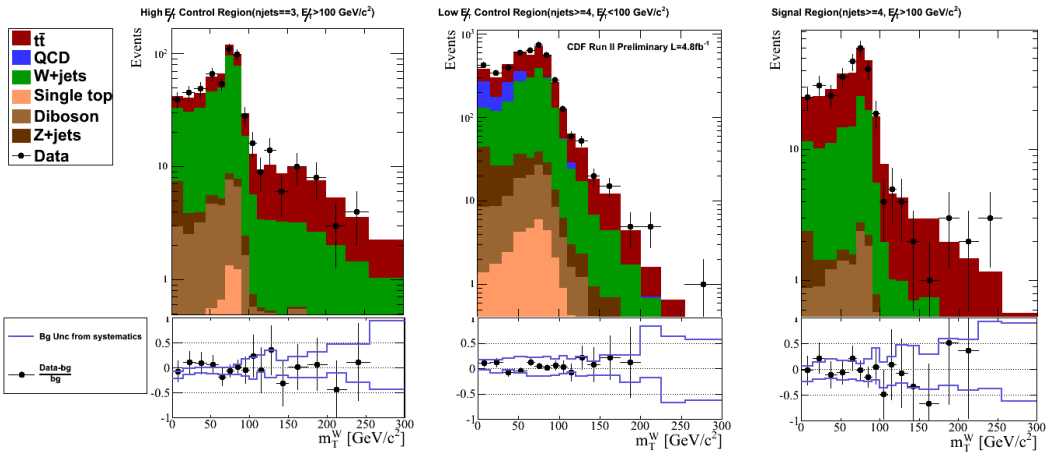

FIG. 4: Backgrounds vs data in mT_W with three different selections.

IV. ANALYSIS STRATEGY

Our signal is different from background in two ways:

- $\not\!\!E_T$: the signal is characterized by an excess of missing transverse energy due to the dark matter particle. We exploit this fact by requiring $\not\!\!E_T > 100$-160 GeV to optimize signal significance. The exact $\not\!\!E_T$ cut varies with the signal point in parameter space $m_{T'}, m_X$, the $\not\!\!E_T$ cuts used are listed in Table II.

- mT_W: in background events, the $\not\!\!E_T >$ comes predominantly from a single neutrino, so there is a strong peak at the W-mass. The signal is more evenly spread in the transverse mass of the leptonically decaying W candidate, mT_W,

$$mT_W \equiv m_T(p_T^l, \not\!\!p_T) = \sqrt{2|p_T^l||\not\!\!p_T|(1 - cos(\Delta\phi(p_T^l, \not\!\!p_T)))}.$$

  This peak in W-mass in background makes it ideal to fit templates of signal and background shapes in mT_W(see Figure 5). We fit templates of the signal and background shapes in mT_W to the observed events in the data, using a binned likelihood and allowing for systematic and statistical fluctuations via template morphing, to extract the most likely signal cross-section.

TABLE I: Number of events for example signal points compared to backgrounds and data for two $\not\!\!E_T$ cuts after initial selection is made.

Cut:	$\not\!\!E_T \geq 100$ GeV/c	$\not\!\!E_T \geq 150$ GeV/c
$T'T' \to ttXX$ [GeV/c^2]		
$m_{T'}, m_X = 300, 90$	$22.9^{+5.8}_{-4.7}$	$4.1^{+2.4}_{-2.1}$
$m_{T'}, m_X = 310, 80$	$22.6^{+4.9}_{-5.1}$	$6.4^{+2.3}_{-2.6}$
$m_{T'}, m_X = 330, 70$	$17.6^{+3.7}_{-3.6}$	$7.3^{+2.5}_{-2.4}$
$m_{T'}, m_X = 350, 1$	$13.1^{+2.7}_{-2.8}$	$6.7^{+2.0}_{-1.9}$
$t\bar{t}$	189^{+54}_{-50}	$26.3^{+11.6}_{-9.8}$
W+jets	105^{+31}_{-14}	$16.6^{+4.5}_{-2.1}$
Single top	1.86 ± 0.2	0.18 ± 0.02
Diboson	9.69 ± 0.1	1.53 ± 0.1
Z+jets	4.00 ± 0.4	0.46 ± 0.05
QCD	0.04 ± 0.01	0.04 ± 0.01
Total Background	310^{+80}_{-64}	45^{+14}_{-11}
Data	309	42

V. RESULTS: LIMITS ON CROSS SECTION

We construct frequentist confidence intervals [7] in the theoretical T' cross section by generating ensembles of simulated experiments that describe expected fluctuations of statistical and systematic uncertainties. For each mass point tested in $(m_{T'}, m_X)$ we list the $\not\!\!E_T$ cut, the 95% confidence level observed upper limits (see Table II) and the expected limits.

We find that the observed limits are consistent with what we would expect if the data were drawn from the standard model.

We plot the numbers from Table II as two 2-dimensional plots(Figure 6b, 6a), a low mass ($m_{T'} = 200 - 280$ GeV plot applicable to the SUSY decay and a high mass ($m_{T'} = 300 - 370$ GeV) plot applicable to the T' decay.

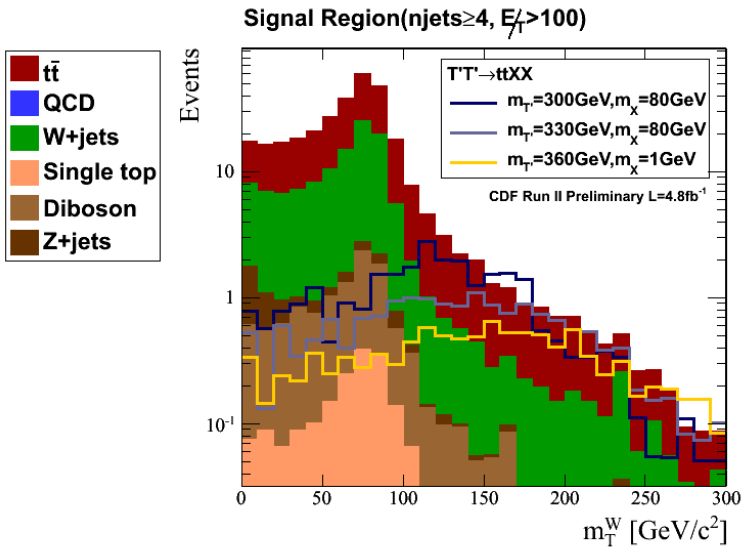

FIG. 5: For three choices of $(m_{T'}, m_X)$, mT_W for signals versus backgrounds in signal region.

VI. RESULTS

We convert limits on the $t\bar{t} + \not{E}_T$ cross sections to exclude $m_{T'}$ up to 360 GeV at 95% confidence level, see Fig. 7

We reinterpret our cross section limits in terms of the supersymmetry decay, $\tilde{t} \to t + \chi^0$. We cannot make any mass exclusion for this decay. We compare median expected and observed limits and theoretical next-to-leading-order (NLO) cross sections(PROSPINO2 [6]) for fixed χ^0 mass; $m_{\chi^0} = 1GeV$(Fig. 8a) and $m_{\chi^0} = 20GeV$(Fig. 8b). Similar plots can me made for different χ^0 masses up to $m_{\chi^0} = 100GeV$.

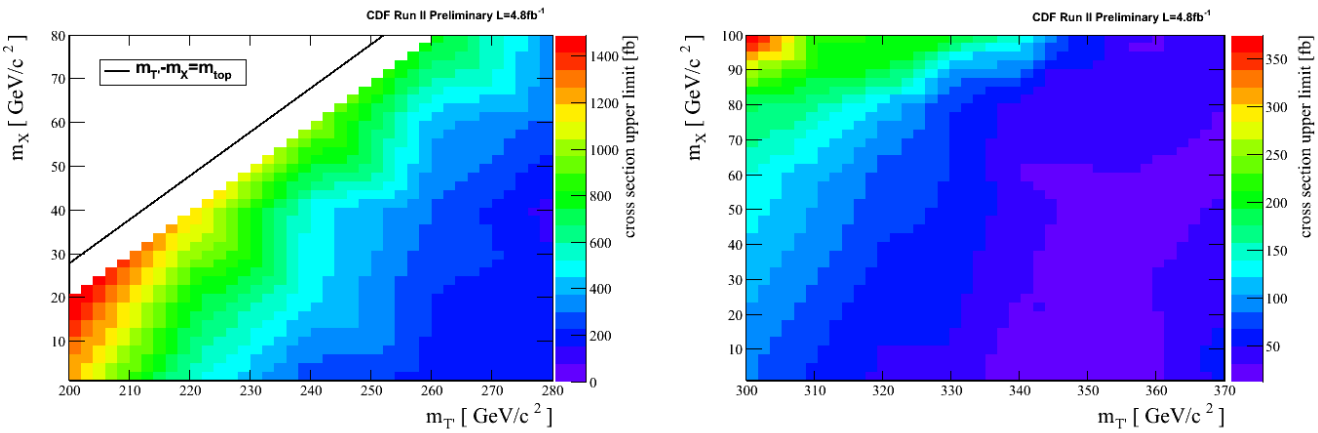

(a) Low mass region.

(b) High mass region.

FIG. 6: 95% C.L. Upper limit on cross-sections..

TABLE II: Expected 95% CL upper limit on $T'\bar{T}'$ production cross-section, σ_{exp}, and observed limit, σ_{obs}, for each signal point in $(m_{T'}, mX)$ tested with the $\not\!\!E_T$ used.

$m_{T'}$,m_X (GeV)	$\not\!\!E_T$ Cut (GeV)	σ_{exp} [pb]	$+\sigma$	$-\sigma$	$+2\sigma$	-2σ	σ_{obs} [pb].
200,1	94	1.31	1.86	0.83	2.34	0.63	1.21
200,20	104	1.78	2.86	1.06	3.71	0.65	1.53
220,1	96	0.78	1.05	0.53	1.28	0.40	0.55
220,20	110	0.89	1.46	0.58	1.90	0.40	0.79
220,40	95	1.40	2.17	0.93	2.94	0.69	1.20
240,1	100	0.39	0.54	0.27	0.68	0.22	0.24
240,20	112	0.44	0.67	0.26	0.89	0.15	0.47
240,40	104	0.61	0.91	0.40	1.17	0.27	0.49
240,60	96	1.39	2.06	0.90	3.92	0.63	1.02
260,1	118	0.23	0.40	0.14	0.53	0.09	0.20
260,20	126	0.27	0.42	0.16	0.59	0.11	0.22
260,40	114	0.36	0.52	0.23	0.67	0.16	0.29
260,60	98	0.49	0.66	0.34	0.83	0.28	0.40
280,1	130	0.16	0.27	0.09	0.38	0.06	0.15
280,20	126	0.18	0.29	0.11	0.36	0.07	0.17
280,40	126	0.17	0.27	0.11	0.35	0.08	0.12
280,60	122	0.27	0.41	0.16	0.58	0.11	0.28
280,80	124	0.40	0.65	0.27	1.06	0.17	0.35
300,100	110	0.34	0.51	0.24	0.82	0.17	0.39
300,90	119	0.26	0.41	0.15	0.67	0.06	0.26
300,80	119	0.20	0.31	0.13	0.42	0.08	0.18
300,70	128	0.19	0.31	0.12	0.42	0.08	0.17
300,60	126	0.16	0.25	0.10	0.34	0.06	0.14
300,30	134	0.13	0.19	0.08	0.31	0.06	0.12
300,1	136	0.11	0.18	0.06	0.28	0.03	0.09
310,100	124	0.23	0.37	0.15	0.83	0.09	0.22
310,90	125	0.19	0.29	0.11	0.46	0.08	0.21
310,80	124	0.16	0.24	0.11	0.30	0.08	0.16
310,1	138	0.10	0.17	0.06	0.27	0.03	0.06
320,90	129	0.15	0.27	0.09	0.49	0.05	0.19
320,80	130	0.15	0.24	0.08	0.44	0.06	0.12

$m_{T'}$,m_X (GeV)	$\not\!\!E_T$ Cut (GeV)	σ_{exp} [pb]	$+\sigma$	$-\sigma$	$+2\sigma$	-2σ	σ_{obs} [pb].
320,70	132	0.12	0.19	0.07	0.28	0.05	0.09
320,60	138	0.11	0.18	0.07	0.31	0.02	0.08
320,30	136	0.09	0.15	0.06	0.21	0.04	0.06
320,1	142	0.09	0.14	0.05	0.20	0.03	0.04
330,100	131	0.14	0.23	0.08	0.40	0.04	0.21
330,90	137	0.13	0.20	0.08	0.29	0.04	0.10
330,80	136	0.11	0.17	0.06	0.30	0.02	0.07
330,70	136	0.10	0.16	0.07	0.25	0.02	0.07
330,60	136	0.09	0.14	0.06	0.21	0.02	0.07
330,30	140	0.09	0.14	0.05	0.20	0.03	0.06
330,1	136	0.08	0.12	0.05	0.17	0.03	0.04
340,100	133	0.11	0.19	0.06	0.35	0.05	0.15
340,80	143	0.10	0.15	0.06	0.29	0.02	0.04
340,70	142	0.09	0.15	0.06	0.30	0.04	0.04
340,60	150	0.08	0.14	0.06	0.24	0.03	0.03
340,30	144	0.07	0.11	0.04	0.16	0.03	0.03
340,1	144	0.07	0.11	0.04	0.15	0.03	0.01
350,110	130	0.09	0.15	0.05	0.35	0.03	0.11
350,100	138	0.10	0.17	0.06	0.47	0.02	0.05
350,70	150	0.08	0.13	0.04	0.36	0.02	0.04
350,50	150	0.07	0.10	0.04	0.17	0.01	0.02
350,30	150	0.07	0.10	0.04	0.16	0.02	0.02
350,1	143	0.07	0.11	0.04	0.21	0.03	0.02
360,110	130	0.09	0.19	0.05	0.21	0.02	0.09
360,100	146	0.08	0.14	0.05	0.29	0.02	0.03
360,70	155	0.07	0.12	0.04	0.28	0.02	0.04
360,30	148	0.06	0.10	0.04	0.20	0.02	0.03
360,1	143	0.06	0.09	0.04	0.25	0.02	0.03
370,100	148	0.07	0.11	0.05	0.19	0.01	0.04
370,70	154	0.07	0.11	0.04	0.24	0.02	0.02
370,1	160	0.06	0.10	0.04	0.19	0.02	0.05

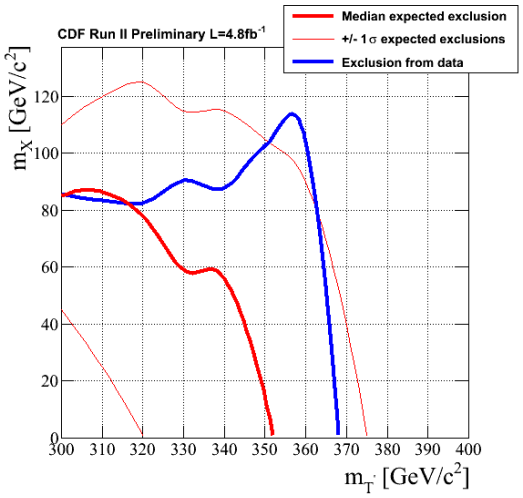

FIG. 7: Observed versus expected exclusion in $(m_{T'}, m_X)$.

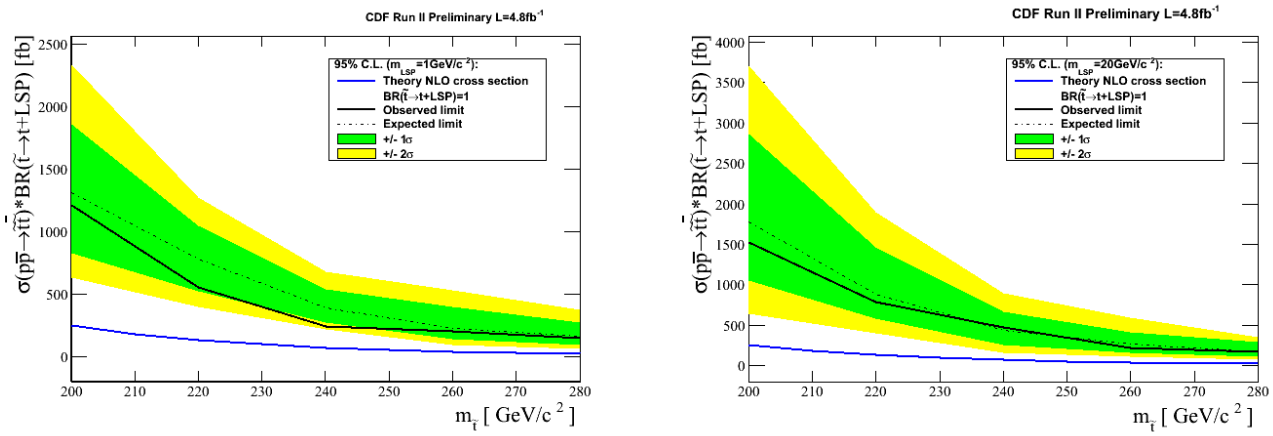

(a) $m_{\chi^0} = 1GeV$ (b) $m_{\chi^0} = 20GeV$

FIG. 8: Comparison of theoretical and observed cross sections for the SUSY decay $\tilde{t} \to t + \chi^0$ for $m_{\chi^0} = 1GeV, 20GeV$.

[1] A. Abulencia *et al.*, J. Phys. G **34**, 2457 (2007).,
[2] J. Alwall *et al.* JHEP 0709:028,(2007).,
[3] J. Feng *et al.* , arXiv:1002.3366 [hep-ph](2010).,
[4] T. Sjostrand *et al.*, Comput. Phys. Commun. 238 135 (2001).
[5] M. M. *et al.*, arXiv:0206293 [hep-ph](2003)
[6] W. Beenaker *et al.*, arXiv:9611232 [hep-ph](1996)
[7] Feldman and Cousins, Phys. Rev. D 57, 3873 (1998).